CASCADE γ-DECAY OF THE ^{193}Os COMPOUND NUCLEUS AND SOME ASPECTS OF DYNAMICS OF CHANGE IN NUCLEAR PROPERTIES BELOW B_n

VALERY.A.BONDARENKO[a], JAROSLAV.HONZÁTKO[b], VALERY. A. KHITROV[c], ANATOLY. M. SUKHOVOJ[c], IVO.TOMANDL[b]

[a] *Nuclear Research Center, LV 2169 Salaspils, Latvia*

[b] *Nuclear Physics Institute, CZ-25068 Řež near Prague, Czech Republic*

[c] *Frank Laboratory of Neutron Physics, Joint Institute for Nuclear Research 141980 Dubna, Russia*

UDC 539.172.4

PACS 25.40.LW, 27.70.+q

arXiv:nucl-ex/0110011v1 18 Oct 2001

Two-step cascades from the $^{192}Os(n_{th},\gamma)^{193}Os$ reaction were studied in $\gamma-\gamma$ coincidence measurement. The decay scheme of ^{193}Os was established up to the excitation energy ~ 3 MeV. The excitation spectrum of intermediate levels of most intense cascades was found to be practically harmonic.

1 Introduction

Nuclear properties in the excitation interval up to the neutron binding energy B_n undergoes radical change: the simplest low-lying levels transform into the Bohr's compound states. The only possibility to study this process in details is provided by the experimental investigation of the two-step γ-cascades proceeding between the neutron resonance and group of low-lying levels. Experimental data on the density and probability of population of the states observed in this process are compared with the theoretical notions. The comparison allows one to reveal the main peculiarities of change in properties of nuclear matter as excitation energy increases. The main details of the analysis of this experiment are described, for example, in [1-3].

2 Experiment

Two-step γ-cascades following thermal neutron capture in ^{190}Os and ^{192}Os were studied by γ-γ coincidence measurements undertaken at the $LWR-15$ reactor in Řež. The measurements

were performed using the spectrometer [4] consisting of two $HPGe$-detectors with the efficiency 20% and 30%. The target consisting of 1200 mg of ^{192}Os and 176 mg of ^{190}Os was used. As the thermal neutron capture cross section [5] equals 13.1 b for ^{190}Os and 3.12 b for ^{192}Os, then this target provided 38% of captures in ^{190}Os and 62% in ^{192}Os.

Unlike other known methods for the study of the process of thermal neutron capture, the sum coincidence method allows one to obtain reliable enough information not only for a monoisotopic target but also for the case of few isotopes with comparable probabilities of neutron capture in them. In the last case, the quality of the experimental data is somewhat worse due to:

(a) increase in the Compton background under the full energy peak in the sum coincidence spectrum caused by a higher-energy cascade belonging to another isotope;

(b) possible overlapping of peaks in the sum coincidence spectrum.

However, a sufficiently high efficiency of detectors and fine energy resolution ($FWHM \simeq 5$ keV for peaks at $E_c = 5 - 6$ MeV in the sum coincidence spectrum) allowed us to obtain the results of acceptable quality in this case, as well.

The main part of the sum coincidence spectrum measured in the experiment is shown in Fig. 1. A relatively large background under the peaks in the region of the neutron binding energy, B_n, is caused by a parasitic neutron capture in $\simeq 3$ mg of Cl contained in the target and surrounding constructions. This component of the background and Compton background at the lower cascade energy $E_c = E_1 + E_2$ determine amplitude and shape of the "noise" line in the intensity distributions of cascades with $E_c = const$. In all there were obtained and analysed 11 such spectra of cascades in ^{193}Os. Each two-step cascade in such spectrum is presented by a pair of peaks with equal areas and widths [6]. The probability of observing a low-intensity cascade is determined only by the amplitude of the "noise" line. The registration threshold, L_c, for individual cascades was determined from an analysis of spectra $E_c = const$ corresponding to background intervals in the sum coincidence spectrum. It was established that L_c linearly increases from 1.5 to 6.0 events per 10^4 decays as the cascade energy changes from 5.6 to 4.5 MeV, respectively.

The data obtained allow one clearly demonstrate spectroscopic possibilities of the method. For this aim all 11 intensity distributions of cascades observed were summed. The part of this summed spectrum for the interval of the quantum energy E_γ from 3.0 to 4.6 MeV is presented in Fig. 2 in function of the energy $E_{ex} = B_n - E_\gamma$ (E_{ex} equals excitation energy of the cascade

intermediate level when E_γ is the energy of the cascade primary transition E_1). Summation leads to accumulation of the primary transition intensities in common peak and intensities of the secondary transitions – in different peaks. Due to low intensity cascades with the secondary transition energy $E_2 >$ MeV are not observed in a given interval of the excitation energy as the peaks, they form continuous distribution. Therefore, every peak in Fig. 2 with the high probability corresponds to one of the levels of ^{193}Os. So, one can see from Fig. 2 that the experimental data allow confident determination of the level energies in ^{193}Os up to $0.5B_n$ as minimum even without the use of the most modern spectrometers.

3 Spectroscopic information

The method to construct a decay scheme using obvious thesis about the constancy of the energy $E_1 = B_n - E_m$ of the primary transition in the cascades with the different total energy $E_1 + E_2 = const$ was described for the first time in [7]. The method uses multi-dimensional distribution in the framework of the maximum likelihood method in order to select probable γ-transitions with equal energy in different spectra. The algorithm gives reliable results [8] even at the mean error in determination of E_1 up to $\simeq 1.5$ keV and number of cascades resolved in spectrum as the pairs of peaks of about 10^3. Corresponding results for ^{193}Os are given in Table 1.

Analysis of the experimental data requires transformation of the peak areas of the resolved cascades into absolute values (in % per decay). However, the direct solution of this problem using, for example, the areas of peaks in the sum coincident spectrum is impossible because of the uncontrollable conditions of the experiment. First of all, this is due to difficulties of determining the number of captures in the target and the absolute efficiency of registration of the cascade in the geometry of the experiment. This problem can be solved by the normalization of relative intensities to the absolute values $A_{\gamma\gamma}$ calculated for most intense cascades by the relation

$$A_{\gamma\gamma} = i_1 \times B_r, \tag{1}$$

where the absolute intensities i_1 of primary transitions are taken from other works, and the branching ratios B_r are determined in a standard way from the codes of coincidences accumulated in this experiment. $A_{\gamma\gamma}$ is the ratio between the intensity of a given cascade and total

intensity of all cascades with $E_1 + E_2 = const$. The use of a maximum large ensemble of reference cascades in the normalization allows one to minimize both statistical and systematical errors of the procedure and practically reduce them to existing errors of i_1.

Unfortunately, there are no reliable data on the absolute intensities of primary transitions for osmium isotopes under consideration. Therefore, we were forced to use the data [9] on relative intensities of γ-transitions following thermal neutron capture in ^{190}Os. For their normalization, we measured the spectrum of γ-rays after thermal neutron capture in the target of natural Os and determined ratios between the peak areas corresponding to γ-transitions with energies 7234, 7793(^{190}Os), 7835(^{188}Os), and 5147 keV (^{191}Os). The absolute intensity of 5147 keV transition belonging to ^{191}Os was determined to be equal $I_1 = 14.4(14)\%$ per decay using absolute intensities [10,11] of three other transitions and data [5,12] on isotopic abundance and thermal neutron capture cross sections. This allowed us to reduce relative intensities of primary transitions in ^{191}Os [9] into the absolute values and determine [13] intensities of the two-step cascades in this nucleus. The coefficient of normalization of relative intensities of the primary transitions in ^{193}Os to absolute values was determined using the ratio of areas of the peaks corresponding to cascades to the ground and three low-lying levels of $^{191,193}Os$ as well as the averaged over corresponding spectra efficiency of registration of the cascades. It was determined to be equal to 0.01077 for the relative intensities of the primary transitions from [14].

The total absolute intensities $I_{\gamma\gamma} = \sum i_{\gamma\gamma}$ of cascades with a fixed sum energy (including those unresolved experimentally) are given in Table 2. The data correspond to the energy detection threshold set at 520 keV which was used to reject annihilation quanta. Nevertheless, the data are suitable for testing the validity of level density and radiative strength function models in the excitation energy range almost up to B_n as it is shown in Table 2.

3.1 Background cascades

Every spectrum – intensity distribution of cascades with a given sum energy contains the following components: (i) desired cascade both in form of pairs of resolved peaks and their superposition – continuous distribution of low amplitude (cascade energy is completely deposited in detectors); (ii) "noise" line resulted from registration of the part of the energy of quanta of cascades with higher energy.

On the average, the contribution of the latter in the spectrum practically equals zero but in some local sections of the spectrum the distortions can be rather considerable. It should be noted that the main distortion is due to the cases of partial absorption of the energy of one cascade transition in detector and complete absorption of the energy of another transition. Subtraction of this Compton background results in appearance of characteristic symmetrical structures of variable sign in spectrum of cascades with less sum energy. As it was shown in [8] these structures manifest themselves when the full energy peaks of high-energy cascades contain more than 1000 events. The use of the numerical algorithm for improvement of energy resolution [6] strengthens this effect. The shape of such structure is determined by the intensity of corresponding individual cascade with higher energy, choice of concrete windows "effect+background" and "background" (Fig. 1) and is due to inevitable discrepancy in positions of these intervals. Of course, similar effect exists and in the standard analysis of $\gamma - \gamma$ coincidences but there it is well "masked".

Precise enough and complete correction of corresponding distortions in the spectra, from which the data of Fig. 2 were obtained, can be calculated. This requires the data on the probability of simultaneous registration of quanta E_1 and E_2 in the full energy peaks for all possible most intense cascades with the higher energy (included cascades in other isotopes and elements situated in neutron beam). This procedure is absolutely necessary if $HPGe$ detectors with the efficiency more than 25-30% are used in the experiment.

3.2 The contribution of ^{191}Os

The contribution of ^{191}Os appears, in particular, in the sum coincidence spectrum as overlapping of full energy peaks related with cascade transitions in ^{193}Os and ^{191}Os. As can be seen from Table 3, such overlapping affects 4 cascade intensity distributions measured in ^{193}Os. It should be noted that this effect was taken into consideration only for final levels of cascades with $J_f \leq 5/2$ because, according to all previous experiments, the intensity of cascades which include even though one quadrupole transition is considerably less than that of cascades with two dipole transitions.

The overlapping of peaks corresponding to different isotopes brings in the necessity to remove well separated, intense cascades belonging to the ^{191}Os isotope from Table 1 and correct the data in Table 2 for its contribution. The correction has sense only if the cascades of ^{193}Os

determine the major part of the area of a given doublet in the sum coincidence spectrum. As a result, the experimentally resolved cascades of ^{191}Os are removed from all 4 spectra.

The removed cascades are attributed to ^{191}Os if within the limits of three standard errors of determination of the intermediate level or γ-transition energy:

(a) intermediate levels with a corresponding energy are not observed in other 7 spectra of ^{193}Os; but

(b) the γ-transition with a close energy is observed in cascade primary transitions of ^{191}Os.

Of course, this procedure does not guarantee an absolute confidence of results. It is, however, more suitable for determination of the level energies than for the determination of decay modes of excited states. A number of cascade transitions observed with a relatively large mean error of determination of their energies ($\Delta E = 0.36$ keV) does not allow one to suggest a more reliable method to exclude cascades belonging to ^{191}Os. Moreover, presently available [15] information on thermal neutron radiative capture spectra of $^{190,192}Os$ is considerably poorer than the data obtained in the reported experiment and cannot be used to solve the problem under consideration.

Correction of the total cascade intensities (Table 2) for the contribution of ^{191}Os can be done in a simpler way. An analysis shows that the low-lying levels of $^{191,193}Os$ with equal J_f^π and the same structure are populated by two-step cascades with approximately equal probabilities. It should be noted that approximate equality of intensities is observed also for the cascades terminating at the levels with different spins $J = 1/2$ or $3/2$ but equal parity. Therefore, the ratio between the contributions of two isotopes in the case of such J_f^π was taken equal to the ratio between the number of neutron captures in ^{190}Os and ^{192}Os. Besides, the intensity of cascades terminating at the $J_f^\pi = 5/2^-$ level of ^{193}Os was assumed to be two times less than the cascade intensity to the $J = 1/2, 3/2$ final levels of ^{191}Os under conditions of equality of numbers of neutron captures in both nuclei.

The results of the procedure are taken into account in the data listed in Table 2. Certainly, it is an approximate solution of the problem. Unresolved doublets represent an insignificant part of the total cascade intensity, however. Hence, one may expect negligible influence of the corresponding error on physical results.

The maximum number of primary transitions belonging to ^{191}Os (but entered in Table 1) can be estimated from frequency distribution of the difference between the energies of the pri-

mary transitions in corresponding spectroscopic data. Such frequency distribution for the 1 keV energy bins in $^{191,193}Os$ is shown in Fig. 3. The enhanced (as compared with neighboring intervals) frequency of observation of the primary transitions with close energy can testify to admixture of the cascades of ^{191}Os in Table 1. Mistaken isotopic identification is observed, probably, for 39(16) transitions from more than 500 primary transitions measured in two isotopes. (Small but statistically significant deviation of the data given in Fig. 3 from zero can be related to error in energy calibration for different Os isotopes). There is rather clear demonstration of reliability of the spectroscopic data obtained in our experiment.

3.3 Comparison with a known decay scheme

Investigation of cascade γ-decay of heavy compound nuclei is a sensitive tool for obtaining spectroscopic information and reliable establishing of a decay scheme up to the excitation energy of 3-4 MeV. The observation confidence of nuclear excited states is mainly determined by the intensity of populating cascades and depends weakly on the excitation energy. For these reasons, the decay scheme of ^{193}Os above $\simeq 1$ MeV established in our experiment seems to be more precise and reliable than obtained earlier.

All observed by us levels of ^{193}Os with $J < 5/2$ are listed in Table 1. The known decay scheme of this nucleus includes only the part of possible levels from those listed in Table 1. This is due to its construction mainly on the basis of spectra of the primary γ-transitions following thermal neutron radiative capture. These spectra, however, were measured at real detection threshold $L_c \simeq 5 \times 10^{-3}$ events per decay. In our experiment there are observed the states of ^{193}Os populated by the cascades with the sum intensity exceeding $2 - 4 \times 10^{-4}$ events per decay. The energy of intermediate levels for the majority of these cascades was determined according to [8] reliably enough, too. In the case of low intensity cascades, quanta ordering was determined [7] only for part of them. Some of the cascades were observed only in one of 11 distributions and one cannot exclude that, possibly, some of the cascades listed in Table 1 can have the low energy primary and high energy secondary transitions.

4 Estimation of possible number of excited states below detection threshold

At zero detection threshold $L_c = 0$ decay scheme would include the main part of excited states of the studied nucleus up to the excitation energy where the mean spacing between the levels is comparable with the widths of peaks (Fig. 2).

Of course, this is impossible. However, the most probable number of levels populated and by the cascades with $< I_{\gamma\gamma} > \leq L_c$ can be estimated if it is taken into account that:

(a) intensity of cascades is the random value with the corresponding average and dispersion;

(b) usually L_c is noticeably less than the mean intensity $< I_{\gamma\gamma} >$ of cascades summed over their final levels (for a given E_i).

Corresponding method of analysis is described in [16]. Its main idea is that one can select such values of three parameters – the set of the mean intensities of cascades with $E1$ or $M1$ primary transitions (in reality - sum of intensities for each intermediate level), the total number of intermediate levels for a given interval of the excitation energy, and L_c – which provide the best reproduction of the cumulative sum of intensities for $< I_{\gamma\gamma} >> L_c$. These parameters of approximation are extrapolated over all region of possible values of cascade intensities on the ground of the condition (b).

Experimental cumulative distribution of $< I_{\gamma\gamma} >$ for some energy intervals of their intermediate levels are compared with the results of the best approximation in Fig. 4. If fluctuations of partial widths of the primary transitions relative to their mean value are described by the Porter-Thomas distribution [17] than the best values of the obtained parameters allow the conclusion that:

1. Table 1 contains more than 99% of the total intensity of cascades populating the levels with $E_i < 3$ MeV and $E_f \leq 890$ keV.

2. The function approximating experimental cumulative sums in the studied nucleus is identical in two possible variants:

(a) or the intensities of cascades with the $E1$ and $M1$ primary transitions and number of their intermediate levels practically are equal;

(b) or the mean intensity of these cascades differs from that of cascades with other type of the transitions by a factor of ≈ 100 and more and their number equals the sum of the probable

number of the intermediate levels according to the variant (a).

3. At the excitation energy above $\simeq 2$ MeV the analysis [16] gives considerably less number of levels than that predicted by the back-shifted Fermi-gas model with the parameters taken from [18].

Available information on the level density is compared in Fig. 5.

It should be noted that a decrease in the model level density used in calculation always leads to an increase in the intensity of the cascades proceeding between the compound state and any low-lying level. The use of the models of the radiative strength functions with the stronger energy dependence also leads to increase in cascade intensity. As it is seen from the Table 2, the calculated cascade intensity is considerably less than the experimental values. This result confirms the conclusions of the analysis [16] that the density of the levels excited in ^{193}Os is considerably less than that predicted by the models which do not take into account the influence on nucleon pairing at $E_{ex} > 2 - 3$ MeV or underestimate it [19]. It should be noted also that ^{193}Os is the first nucleus where the calculated cascade intensities are stronger affected by choice the model of the radiative strength functions than by choice of the level density model. But on the whole, theoretical notions of the level density and radiative strength functions for ^{193}Os are to be developed completely in the same direction as that earlier obtained [22] for other nuclei.

5 Probable dominant component of the wave functions of the intermediate levels of most intense cascades

According to the modern theoretical notions, the wave function structure of any excited states is determined by co-existence and interaction between the fermion (quasiparticles) and boson (phonons) excitations. With the excitation energy a nucleus transits from practically mono-component excitations of the mentioned types to the mixed (quasiparticles $\otimes$ phonons) states with rather different [23] degree of their fragmentation. This process should be investigated in details but there is no adequate experimental methods to study the structure of the wave functions above the excitation energy of 1-3 MeV.

Nevertheless, some information on the probable dominant components of wave functions of heavy deformed nuclei can be obtained. The authors of [24] suggested to search for the regularity in the excitation spectra of the intermediate levels of most intense cascades by means of auto-correlation analysis of the smoothed distributions of the sum cascade intensities from

Table 1. Intensities were smoothed by means of the Gaussian function: $F(E) = \sum_E I_{\gamma\gamma} \times exp(-0.5(\Delta E/\sigma)^2)$. The distribution of this type smoothed with the parameter $\sigma = 25$ keV is given in Fig. 6 and the values of the auto-correlation function

$$A(T) = \sum_E F(E) \times F(E+T) \times F(E+2T). \quad (2)$$

for different selection thresholds of intense cascades are shown in Fig. 7. As it was shown in [25] such analysis cannot give unique value of the equidistant period T even for the simulated spectra (for example, for 25 "bands" consisting from 4 levels with slightly distorted equidistant period) and provide estimation of the confidence level of the observed effect. In principle, both problems can be solved in the experiments on the study of the two-step cascades in different resonances of the same nucleus. But some grounds to state that the regularity really exists can be obtained from a comparison of the most probable equidistant periods in different nuclei. The set of the probable equidistant periods obtained so far (Fig. 8) allows an assumption that the T value is approximately proportional to the number of boson pairs of the unfilled nuclear shells. This allows one to consider the effect at the level of working hypothesis.

The regularity in the excitation spectra testifies to the harmonic nuclear vibrations. Thus, one can assume that the structure of the intermediate levels of the studied cascades contains considerable components of the rather weakly fragmented states like multi-quasiparticle excitations $\otimes$ phonon or several phonons. This provides logical explanation of serious decrease in the observed level density as compared with the predictions of the non-interacting Fermi-gas model: nuclear excitation energy concentrates on phonos but quasiparticles up to the $\simeq$ 2 MeV are populate weakly or very weakly due to insufficiency of energy for breaking of paired nucleons.

6 Influence of structure of final level on cascade intensity

The structure of some levels of ^{193}Os is known: the ground state and level E_f=72 keV are the members of the rotational band $[Nn_z\Lambda] = [512]\downarrow$, levels E_f=41, 102, and, probably, 295 keV belong to the band $[510]\uparrow$. It is seen from the Table 2 that the ratio between the experimental and calculated cascades intensities amounts on the average to 1.9 and 2.7 in the first and second cases, respectively. This discrepancy, as that observed earlier in other even-odd compound nuclei, may be related [2] with the influence of the structure of the cascade final level on mean probability of the cascade.

7 Conclusion

Information on two-step γ-cascades for a number of nuclei from the mass range $114 \leq A \leq 200$ (see, for example, [26]) from thermal neutron capture experiments forms a basis for study of the characteristics of the γ-decay process.

The results indicate necessity to modify model notions of the properties of the excited states of the heavy nuclei. The obtained information demonstrates that more correct description of the process under study requires more detailed accounting for co-existence and interaction of superfluid and normal phases of nuclear matter by the nuclear models. Achievement of complete correspondence between the observed and calculated parameters of nuclear reactions, for instance, neutron-induced reaction is impossible. This concerns, partially, the total radiative widths of neutron resonances and γ-spectrum .

This work was supported by GACR under contract No. 202/97/K038 and by RFBR Grant No. 99-02-17863.

Table 1.
A list of absolute intensities (per 10^2 decays), $i_{\gamma\gamma}$, of measured two-step cascades and energies, E_1 and E_2, of the cascade transitions, E_i is the energy of the intermediate levels.

E_1,keV	E_i, keV	E_2, keV	$i_{\gamma\gamma}$
5277.00	306.90(10)	306.90	0.326(16)
		265.42	2.209(52)
		204.17	0.374(13)
5033.00	550.90(20)	448.17	0.032(4)
5010.70	573.20(20)	266.12	0.055(12)
4996.30	587.60(10)	353.74	0.041(6)
4908.70	675.20(10)	633.72	0.017(4)
		572.47	0.013(4)
4795.40	788.50(10)	788.50	0.025(5)
4694.50	889.40(10)	889.40	1.031(19)
		847.92	0.087(9)
		816.50	0.165(8)
		786.67	0.821(27)
		655.54	0.183(16)
		582.32	0.207(45)
4617.00	966.90(18)	671.22	0.014(4)
		567.88	0.011(3)
4530.20	1053.70(20)	1053.70	0.312(8)
		1012.22	0.688(15)
		980.80	0.065(5)
		950.97	5.791(49)
		746.62	0.500(38)
4499.40	1084.50(45)	1043.02	0.033(4)
		788.82	0.070(9)
4413.20	1170.70(40)	1170.70	0.097(8)
		1129.22	0.806(24)
		1097.80	0.171(10)
		1067.97	0.226(10)
		936.84	0.176(16)
		875.02	0.161(12)
		863.62	0.034(11)
		714.93	0.030(6)
		461.50	0.083(7)

E_1,keV	E_i, keV	E_2, keV	$i_{\gamma\gamma}$
4405.60	1178.30(20)	1178.30	0.717(19)
		1136.82	0.029(6)
		1105.40	0.107(8)
		1075.57	0.342(11)
		871.22	0.097(15)
		779.28	0.020(7)
		722.53	0.131(9)
4398.50	1185.40(20)	1082.67	0.023(6)
4378.70	1205.20(50)	1163.72	0.076(9)
		1102.47	0.097(6)
4366.40	1217.50(26)	1217.50	0.176(9)
		1176.02	0.593(21)
		1144.60	0.090(8)
		1114.77	0.433(13)
		921.82	0.024(7)
		910.42	0.066(12)
		818.48	0.094(10)
		761.73	0.072(6)
4358.20	1225.70(41)	1184.22	0.026(6)
		1152.80	0.020(6)
		769.93	0.448(16)
4339.30	1244.60(39)	1203.12	0.015(6)
		788.83	0.062(6)
4316.60	1267.30(27)	1164.57	0.093(10)
4301.00	1282.90(20)	1282.90	0.170(9)
		1241.42	0.100(6)
		1210.00	0.036(4)
		1180.17	0.068(8)
		987.22	0.032(7)
		883.88	0.119(14)
		573.70	0.031(6)
4295.30	1288.60(10)	1288.60	0.630(18)
		1247.12	0.127(6)

Table 1 (continued)

E_1,keV	E_i, keV	E_2, keV	$i_{\gamma\gamma}$
		1215.70	0.014(4)
		1185.87	0.040(8)
		992.92	0.064(7)
		889.58	0.081(11)
		579.40	0.063(6)
		399.12	0.115(12)
4250.40	1333.50(30)	1333.50	0.060(5)
		1292.02	0.083(6)
		1260.60	0.017(4)
		1230.77	0.448(17)
		1099.64	0.112(14)
		1037.82	0.021(7)
		934.48	0.026(9)
		877.73	0.029(12)
4224.30	1359.60(30)	1359.60	0.045(5)
		1318.12	0.059(5)
		1286.70	0.035(4)
		1256.87	0.108(10)
		1125.74	0.851(37)
		1063.92	0.047(5)
		1052.52	0.065(6)
		960.58	0.144(15)
		903.83	0.095(14)
4200.30	1383.60(30)	1076.52	0.029(6)
4197.90	1386.00(80)	1386.00	0.754(18)
		1344.52	0.140(9)
		1313.10	0.029(5)
		1283.27	0.019(4)
		1090.32	0.027(5)
		1078.92	0.096(7)
4185.70	1398.20(36)	1398.20	0.069(8)
		1325.30	0.032(5)

E_1,keV	E_i, keV	E_2, keV	$i_{\gamma\gamma}$
4183.90	1400.00(30)	1400.00	0.034(6)
		1358.52	0.017(6)
		1297.27	0.199(8)
		1092.92	0.043(6)
4165.90	1418.00(26)	1418.00	0.066(6)
		1376.52	0.016(5)
		1345.10	0.045(5)
		1122.32	0.022(5)
4149.90	1434.00(70)	1434.00	0.014(5)
4137.40	1446.50(57)	1373.60	0.112(6)
4086.50	1497.40(45)	1497.40	0.018(5)
4079.80	1504.10(41)	1504.10	0.024(5)
		1401.37	0.025(6)
		1270.24	0.070(6)
		1048.33	0.038(9)
4068.30	1515.60(100)	1515.60	0.021(5)
		1474.12	0.051(6)
		1412.87	0.085(8)
		1219.92	0.054(8)
		1208.52	0.200(11)
		1116.58	0.083(11)
		1059.83	0.060(10)
4060.40	1523.50(40)	1523.50	0.069(6)
		1482.02	0.067(6)
		1420.77	0.207(11)
		1216.42	0.207(11)
4053.60	1530.30(29)	1488.82	0.248(10)
		1427.57	0.327(13)
		1234.62	0.037(8)
		1223.22	0.062(6)
		1131.28	0.035(11)
4028.10	1555.80(20)	1514.32	0.060(6)

Table 1 (continued)

E_1,keV	E_i, keV	E_2, keV	$i_{\gamma\gamma}$
		1248.72	0.035(6)
3993.00	1590.90(80)	1590.90	0.222(11)
		1549.42	0.040(5)
		1518.00	0.049(5)
		1488.17	0.087(8)
		1295.22	0.046(6)
		1283.82	0.139(12)
3980.70	1603.20(32)	1603.20	0.046(6)
		1561.72	0.671(17)
		1530.30	0.023(5)
		1500.47	0.610(17)
		1369.34	0.029(6)
		1307.52	0.178(10)
		1296.12	0.272(16)
		1204.18	0.212(16)
		1147.43	0.155(14)
3923.60	1660.30(30)	1618.82	0.017(5)
3903.60	1680.30(42)	1373.22	0.024(8)
3900.60	1683.30(17)	1683.30	0.091(9)
		1641.82	0.350(12)
		1610.40	0.021(5)
		1580.57	0.445(15)
		1449.44	0.250(12)
		1387.62	0.138(9)
		1376.22	0.072(9)
		974.10	0.042(6)
3861.40	1722.50(30)	1722.50	0.019(5)
		1619.77	0.017(6)
		1426.82	0.018(6)
3852.30	1731.60(33)	842.12	0.058(9)
3846.30	1737.60(60)	1634.87	0.025(6)
3839.00	1744.90(90)	1672.00	0.016(5)
		1289.13	0.016(5)

E_1,keV	E_i, keV	E_2, keV	$i_{\gamma\gamma}$
3829.70	1754.20(110)	1754.20	0.016(5)
		1520.34	0.016(4)
3823.50	1760.40(20)	1657.67	0.047(8)
		1526.54	0.014(4)
3818.80	1765.10(85)	1723.62	0.074(6)
		1692.20	0.027(5)
		1662.37	0.108(8)
		1531.24	0.102(6)
		1458.02	0.117(8)
		1366.08	0.056(5)
		1309.33	0.048(5)
		1055.90	0.025(6)
3800.10	1783.80(90)	1783.80	0.065(6)
		1742.32	0.112(7)
		1710.90	0.033(5)
		1549.94	0.129(7)
		1488.12	0.025(5)
		1476.72	0.035(6)
		1384.78	0.035(5)
		1328.03	0.030(5)
3788.10	1795.80(43)	1693.07	0.021(6)
		1561.94	0.019(4)
3785.00	1798.90(50)	1565.04	0.030(4)
3781.90	1802.00(75)	1760.52	0.022(5)
3778.80	1805.10(34)	1805.10	0.026(5)
3757.20	1826.70(90)	1826.70	0.018(5)
		1753.80	0.014(5)
3752.80	1831.10(28)	1831.10	0.029(5)
		1789.62	0.037(5)
		1758.20	0.032(5)
		1597.24	0.037(4)
		1535.42	0.027(5)
		1524.02	0.018(6)

Table 1 (continued)

E_1,keV	E_i, keV	E_2, keV	$i_{\gamma\gamma}$
		1432.08	0.020(4)
		1375.33	0.022(5)
3745.60	1838.30(20)	1765.40	0.021(5)
		1735.57	0.025(6)
		1604.44	0.073(5)
		1531.22	0.399(15)
		1129.10	0.051(9)
3736.80	1847.10(52)	1847.10	0.026(6)
		1805.62	0.065(6)
		1774.20	0.024(5)
		1744.37	0.080(8)
		1551.42	0.019(5)
		1540.02	0.028(6)
		1448.08	0.073(5)
		1137.90	0.047(9)
3730.30	1853.60(92)	1619.74	0.016(4)
3721.20	1862.70(80)	1759.97	0.029(6)
3709.30	1874.60(45)	1874.60	0.031(10)
3695.00	1888.90(84)	1816.00	0.029(5)
		1786.17	0.032(8)
		1489.88	0.024(5)
		1179.70	0.037(9)
3691.30	1892.60(27)	1892.60	0.025(10)
		1851.12	0.040(5)
		1819.70	0.040(5)
		1436.83	0.021(6)
3675.30	1908.60(35)	1867.12	0.015(5)
		1509.58	0.032(6)
		1452.83	0.025(6)
3668.60	1915.30(43)	1915.30	0.029(10)
		1873.82	0.411(12)
		1812.57	0.030(6)
		1681.44	0.294(10)

E_1,keV	E_i, keV	E_2, keV	$i_{\gamma\gamma}$
		1608.22	0.416(16)
		1516.28	0.019(6)
		1459.53	0.022(6)
3662.70	1921.20(30)	1848.30	0.013(5)
		1818.47	0.030(6)
3651.80	1932.10(60)	1890.62	0.028(5)
		1859.20	0.089(5)
3648.80	1935.10(16)	1935.10	0.023(10)
		1832.37	0.082(6)
		1536.08	0.023(5)
3645.30	1938.60(44)	1938.60	0.321(24)
		1897.12	0.048(5)
3634.90	1949.00(42)	1641.92	0.018(6)
3629.10	1954.80(20)	1852.07	0.355(11)
		1720.94	0.022(4)
		1647.72	0.016(6)
		1499.03	0.017(5)
3606.50	1977.40(90)	1935.92	0.037(5)
		1743.54	0.030(4)
		1670.32	0.107(8)
		1578.38	0.021(5)
		1087.92	0.054(10)
3600.50	1983.40(22)	1983.40	0.160(16)
		1910.50	0.067(5)
		1880.67	0.070(6)
		1749.54	0.015(4)
		1687.72	0.020(6)
3594.10	1989.80(60)	1755.94	0.020(4)
3581.80	2002.10(28)	1960.62	0.210(11)
		1929.20	0.087(6)
		1768.24	0.048(5)
		1706.42	0.039(6)
		1695.02	0.040(6)

Table 1 (continued)

E_1,keV	E_i, keV	E_2, keV	$i_{\gamma\gamma}$
		1603.08	0.025(6)
3570.30	2013.60(37)	1972.12	0.123(9)
		1910.87	0.032(6)
		1779.74	0.015(4)
		1706.52	0.051(6)
		1557.83	0.017(6)
		1124.12	0.094(10)
3563.10	2020.80(80)	1786.94	0.022(4)
		1713.72	0.021(6)
3559.60	2024.30(55)	1982.82	0.027(6)
3546.50	2037.40(80)	1803.54	0.030(5)
		1741.72	0.022(6)
		1730.32	0.018(5)
		1581.63	0.030(6)
3544.00	2039.90(70)	2039.90	0.043(5)
		1732.82	0.021(5)
3535.80	2048.10(30)	2048.10	0.141(8)
		1945.37	0.049(8)
		1814.24	0.049(6)
		1741.02	0.040(5)
3533.10	2050.80(80)	1816.94	0.023(5)
		1755.12	0.046(6)
		1651.78	0.046(5)
3530.40	2053.50(85)	1950.77	0.080(10)
3524.20	2059.70(20)	2018.22	0.018(6)
3519.80	2064.10(16)	2064.10	0.039(5)
		2022.62	0.051(7)
		1991.20	0.076(6)
		1961.37	0.097(10)
		1757.02	0.053(5)
		1665.08	0.059(6)
		1608.33	0.049(6)

E_1,keV	E_i, keV	E_2, keV	$i_{\gamma\gamma}$
		1354.90	0.019(7)
3516.30	2067.60(8)	2067.60	0.030(5)
		1833.74	0.082(6)
		1760.52	0.043(5)
		1178.12	0.052(8)
3505.60	2078.30(50)	2078.30	0.039(5)
		2036.82	0.295(12)
		2005.40	0.031(5)
		1844.44	0.052(5)
		1782.62	0.020(6)
		1771.22	0.115(7)
		1679.28	0.027(5)
		1622.53	0.043(6)
		1369.10	0.026(7)
		1188.82	0.032(8)
3502.80	2081.10(46)	2008.20	0.054(5)
		1978.37	0.042(8)
		1785.42	0.027(6)
		1774.02	0.035(5)
		1682.08	0.052(6)
		1625.33	0.025(6)
3491.00	2092.90(20)	2092.90	0.020(5)
		2020.00	0.022(5)
		1990.17	0.038(8)
		1859.04	0.032(5)
		1797.22	0.038(6)
		1693.88	0.111(7)
		1203.42	0.028(8)
3485.90	2098.00(48)	2098.00	0.024(5)
		2056.52	0.021(6)
		1995.27	0.021(8)
		1864.14	0.045(5)

Table 1 (continued)

E_1,keV	E_i, keV	E_2, keV	$i_{\gamma\gamma}$
		1802.32	0.023(6)
		1790.92	0.020(5)
		1388.80	0.047(7)
		1208.52	0.045(8)
3480.50	2103.40(40)	2061.92	0.018(6)
		1807.72	0.018(6)
3475.80	2108.10(80)	1874.24	0.022(6)
3472.20	2111.70(70)	2111.70	0.024(5)
		1222.22	0.034(8)
3468.00	2115.90(50)	2074.42	0.032(6)
3459.80	2124.10(32)	2021.37	0.046(8)
		1890.24	0.022(4)
3457.50	2126.40(32)	2084.92	0.032(6)
		1819.32	0.032(5)
3450.90	2133.00(67)	2133.00	0.030(5)
		2030.27	0.017(6)
		1899.14	0.054(7)
		1837.32	0.037(5)
		1733.98	0.037(5)
		1677.23	0.054(6)
		1243.52	0.168(9)
3449.70	2134.20(40)	2134.20	0.021(5)
		1900.34	0.048(6)
		1827.12	0.086(6)
3440.40	2143.50(42)	2040.77	0.015(6)
3433.30	2150.60(52)	2109.12	0.018(7)
		1854.92	0.023(5)
3430.10	2153.80(60)	2051.07	0.061(8)
		1858.12	0.039(5)
3426.80	2157.10(10)	2157.10	0.030(5)
		1850.02	0.028(5)
3420.20	2163.70(50)	2090.80	0.042(5)
		1929.84	0.026(4)

E_1,keV	E_i, keV	E_2, keV	$i_{\gamma\gamma}$
		1707.93	0.021(6)
3415.20	2168.70(40)	2168.70	0.111(8)
		2127.22	0.187(11)
		2065.97	0.017(6)
		1873.02	0.023(5)
		1861.62	0.026(5)
		1769.68	0.049(5)
3405.80	2178.10(10)	1288.62	0.042(11)
3402.60	2181.30(80)	2139.82	0.056(7)
		2108.40	0.019(5)
3398.50	2185.40(50)	2143.92	0.017(6)
		2082.67	0.146(10)
		1878.32	0.023(11)
		1295.92	0.048(11)
3391.50	2192.40(22)	2150.92	0.063(7)
		2089.67	0.078(8)
		1483.20	0.029(8)
3388.90	2195.00(31)	2092.27	0.046(8)
		1887.92	0.216(19)
		1795.98	0.016(5)
		1305.52	0.082(11)
3378.80	2205.10(35)	2102.37	0.040(6)
		1806.08	0.018(5)
3365.30	2218.60(25)	2218.60	0.030(5)
		1984.74	0.073(6)
		1922.92	0.033(5)
		1819.58	0.014(5)
3361.90	2222.00(26)	2222.00	0.014(5)
		1988.14	0.024(5)
3358.80	2225.10(30)	2183.62	0.251(12)
		1929.42	0.026(5)
3353.30	2230.60(28)	2230.60	0.023(5)
		2127.87	0.042(6)

Table 1 (continued)

E_1,keV	E_i, keV	E_2, keV	$i_{\gamma\gamma}$
3349.30	2234.60(70)	2234.60	0.021(5)
3344.00	2239.90(50)	2198.42	0.021(6)
3337.60	2246.30(70)	2204.82	0.029(6)
3334.80	2249.10(20)	2176.20	0.152(9)
		2146.37	0.067(8)
		1942.02	0.380(25)
		1850.08	0.088(7)
		1359.62	0.058(11)
3334.70	2249.20(95)	1540.00	0.061(12)
3333.00	2250.90(70)	2250.90	0.602(26)
		2209.42	0.028(6)
3328.00	2255.90(20)	2153.17	0.021(6)
		1948.82	0.031(11)
3325.50	2258.40(40)	2258.40	0.024(9)
		1859.38	0.022(5)
3305.20	2278.70(20)	2205.80	0.028(5)
		2175.97	0.021(6)
		1983.02	0.020(6)
3298.50	2285.40(40)	2182.67	0.055(6)
3293.40	2290.50(30)	2290.50	0.020(8)
		2249.02	0.033(5)
3289.60	2294.30(31)	2294.30	0.021(8)
3286.60	2297.30(60)	2255.82	0.032(5)
		2224.40	0.033(5)
		2194.57	0.017(6)
3273.90	2310.00(15)	2310.00	0.052(14)
		2268.52	0.045(5)
		2076.14	0.035(16)
3268.00	2315.90(78)	2315.90	0.026(9)
		2274.42	0.056(5)
		2020.22	0.022(6)
		2008.82	0.020(8)

E_1,keV	E_i, keV	E_2, keV	$i_{\gamma\gamma}$
		1860.13	0.064(8)
3263.40	2320.50(27)	2320.50	0.107(13)
		2217.77	0.076(6)
		2086.64	0.078(7)
		2024.82	0.020(6)
3257.80	2326.10(90)	2326.10	0.066(10)
		2284.62	0.048(5)
		2223.37	0.291(11)
		2030.42	0.027(6)
3251.30	2332.60(29)	2291.12	0.016(5)
		2229.87	0.017(6)
3243.80	2340.10(42)	2298.62	0.026(5)
3241.00	2342.90(80)	2301.42	0.029(5)
		2240.17	0.055(6)
3235.90	2348.00(24)	2348.00	0.032(5)
		2306.52	0.110(6)
		2245.27	0.055(6)
		2114.14	0.029(6)
3233.50	2350.40(40)	2043.32	0.019(8)
3223.00	2360.90(75)	2127.04	0.021(6)
3219.70	2364.20(37)	2364.20	0.024(5)
		2261.47	0.025(6)
3215.90	2368.00(29)	2326.52	0.052(6)
		2265.27	0.093(8)
		2134.14	0.172(11)
		2060.92	0.019(8)
		1478.52	0.064(8)
3210.80	2373.10(34)	2373.10	0.016(5)
3202.90	2381.00(27)	2381.00	0.043(5)
		2308.10	0.019(5)
		2073.92	0.020(8)
		1491.52	0.033(8)

Table 1 (continued)

E_1,keV	E_i, keV	E_2, keV	$i_{\gamma\gamma}$
3194.80	2389.10(43)	2389.10	0.153(10)
		2347.62	0.026(6)
		2286.37	0.055(6)
		2155.24	0.020(5)
		2093.42	0.023(6)
		1990.08	0.022(9)
		1933.33	0.028(10)
		1499.62	0.065(8)
3187.60	2396.30(31)	2396.30	0.046(5)
3176.90	2407.00(47)	2407.00	0.024(5)
		2365.52	0.072(6)
		2304.27	0.080(8)
		2111.32	0.041(7)
		2007.98	0.031(9)
3169.90	2414.00(85)	2372.52	0.021(6)
3162.90	2421.00(27)	2379.52	0.070(7)
		2021.98	0.017(5)
		1531.52	0.042(9)
3157.10	2426.80(40)	2426.80	0.055(6)
		2324.07	0.036(6)
		2192.94	0.017(5)
3152.60	2431.30(80)	2431.30	0.047(6)
		2328.57	0.093(10)
3151.10	2432.80(40)	2432.80	0.019(5)
		2391.32	0.155(9)
		2330.07	0.019(8)
		2125.72	0.037(9)
		2033.78	0.019(5)
3146.20	2437.70(40)	2396.22	0.017(6)
3141.40	2442.50(52)	2442.50	0.032(5)
3136.90	2447.00(100)	2405.52	0.051(6)
		2151.32	0.019(6)
3133.80	2450.10(55)	2377.20	0.015(5)
		2347.37	0.019(6)
3125.40	2458.50(20)	2355.77	0.027(6)
		2151.42	0.017(6)
3122.20	2461.70(50)	2461.70	0.027(5)
		2227.84	0.110(7)
		2154.62	0.031(6)
3116.20	2467.70(50)	2426.22	0.052(6)
		2364.97	0.021(6)
		2233.84	0.022(5)
		2160.62	0.019(6)
		2068.68	0.020(5)
		2011.93	0.025(10)
3113.50	2470.40(29)	2470.40	0.025(8)
		2163.32	0.025(6)
3099.60	2484.30(20)	2442.82	0.057(6)
		2381.57	0.023(6)
		2250.44	0.035(5)
3097.20	2486.70(65)	2179.62	0.016(6)
3094.30	2489.60(25)	2489.60	0.044(6)
		2386.87	0.021(8)
		2182.52	0.024(6)
		2090.58	0.033(5)
3088.90	2495.00(70)	2422.10	0.070(5)
		2261.14	0.015(5)
		2187.92	0.024(5)
		2039.23	0.063(7)
3084.20	2499.70(24)	2499.70	0.027(6)
		2458.22	0.077(15)
		2426.80	0.027(5)
		2396.97	0.021(8)
		2265.84	0.025(5)

Table 1 (continued)

E_1,keV	E_i, keV	E_2, keV	$i_{\gamma\gamma}$
		2204.02	0.051(6)
3080.40	2503.50(32)	2503.50	0.019(6)
3077.60	2506.30(100)	2433.40	0.045(5)
3075.60	2508.30(25)	2508.30	0.083(8)
		2466.82	0.034(7)
		2405.57	0.027(8)
		2274.44	0.073(6)
		2201.22	0.022(5)
		2109.28	0.020(5)
		2052.53	0.044(6)
3072.10	2511.80(70)	2511.80	0.031(6)
		2438.90	0.040(5)
		2409.07	0.070(10)
		2204.72	0.023(6)
		2112.78	0.086(6)
		2056.03	0.028(6)
3069.80	2514.10(6)	2514.10	0.026(6)
		2472.62	0.023(7)
		2280.24	0.039(5)
		2218.42	0.020(6)
		2207.02	0.027(6)
3064.70	2519.20(50)	2519.20	0.032(6)
		2477.72	0.032(7)
		2446.30	0.018(5)
		2416.47	0.034(8)
		2063.43	0.035(6)
3055.50	2528.40(50)	2528.40	0.015(6)
		2455.50	0.030(5)
		2425.67	0.019(8)
		2072.63	0.026(6)
3053.00	2530.90(40)	2223.82	0.021(6)
3050.20	2533.70(70)	2533.70	0.105(9)
		2299.84	0.058(5)
3042.10	2541.80(40)	2541.80	0.015(6)
		2468.90	0.022(6)
		2439.07	0.076(10)
		2307.94	0.052(5)
		2234.72	0.051(6)
		2086.03	0.051(6)
3035.70	2548.20(60)	2445.47	0.044(8)
		2314.34	0.093(6)
		2252.52	0.029(7)
3032.60	2551.30(90)	2551.30	0.144(10)
3029.30	2554.60(80)	2554.60	0.016(6)
		2247.52	0.019(6)
3025.80	2558.10(44)	2516.62	0.081(7)
		2251.02	0.022(6)
3023.50	2560.40(30)	2487.50	0.030(5)
		2457.67	0.030(8)
		2326.54	0.035(5)
		2253.32	0.040(6)
3016.80	2567.10(15)	2567.10	0.070(9)
		2525.62	0.040(6)
		2494.20	0.057(6)
		2260.02	0.042(6)
		2168.08	0.034(6)
		2111.33	0.047(6)
3005.90	2578.00(50)	2344.14	0.027(9)
3003.80	2580.10(34)	2538.62	0.032(6)
		2507.20	0.045(5)
		2477.37	0.158(10)
		2346.24	0.052(9)

Table 1 (continued)

E_1,keV	E_i, keV	E_2, keV	$i_{\gamma\gamma}$
		2284.42	0.024(6)
		2124.33	0.037(6)
2998.90	2585.00(85)	2585.00	0.018(6)
		2543.52	0.030(6)
2986.50	2597.40(30)	2597.40	0.067(9)
		2363.54	0.019(5)
2981.10	2602.80(80)	2602.80	0.021(6)
		2561.32	0.029(7)
		2529.90	0.043(5)
		2203.78	0.028(6)
		2147.03	0.022(6)
2977.00	2606.90(32)	2504.17	0.023(6)
2972.60	2611.30(25)	2611.30	0.020(6)
		2569.82	0.233(13)
		2508.57	0.049(6)
		2315.62	0.048(6)
		1902.10	0.030(8)
2969.20	2614.70(14)	2380.84	0.028(5)
2954.60	2629.30(24)	2526.57	0.044(6)
		2322.22	0.015(6)
2951.60	2632.30(10)	2632.30	0.049(8)
		2590.82	0.041(7)
		2529.57	0.030(6)
2946.10	2637.80(30)	2637.80	0.018(6)
		2596.32	0.039(6)
		2535.07	0.015(6)
2927.30	2656.60(42)	2656.60	0.043(6)
		2615.12	0.057(7)
		2553.87	0.040(8)
2922.10	2661.80(35)	2354.72	0.020(6)
2912.50	2671.40(30)	2671.40	0.125(11)
		2629.92	0.077(7)
		2598.50	0.040(6)

E_1,keV	E_i, keV	E_2, keV	$i_{\gamma\gamma}$
		2568.67	0.057(11)
		2437.54	0.035(6)
		2364.32	0.060(6)
2904.30	2679.60(50)	2679.60	0.030(8)
		2638.12	0.035(6)
		2445.74	0.022(6)
		2280.58	0.072(6)
2896.80	2687.10(14)	2645.62	0.032(6)
		2614.20	0.026(6)
2893.70	2690.20(35)	2648.72	0.028(6)
		2456.34	0.033(7)
2890.00	2693.90(52)	2621.00	0.026(6)
		2591.17	0.019(6)
2886.90	2697.00(50)	2594.27	0.047(8)
		2463.14	0.030(7)
		2401.32	0.051(8)
		2389.92	0.019(6)
2884.40	2699.50(70)	2699.50	0.076(8)
		2658.02	0.041(7)
		2626.60	0.024(6)
		2596.77	0.101(10)
		2465.64	0.024(7)
		2300.48	0.026(5)
2880.20	2703.70(75)	2662.22	0.046(7)
		2600.97	0.032(8)
		2469.84	0.076(9)
		2396.62	0.045(6)
		2304.68	0.016(5)
2875.00	2708.90(65)	2475.04	0.066(8)
		2413.22	0.022(7)
2869.10	2714.80(14)	2480.94	0.022(6)
		2407.72	0.032(6)
2867.00	2716.90(42)	2409.82	0.029(6)

Table 1 (continued)

E_1,keV	E_i, keV	E_2, keV	$i_{\gamma\gamma}$
2863.70	2720.20(60)	2720.20	0.025(6)
		2678.72	0.057(12)
		2647.30	0.026(6)
		2486.34	0.026(6)
		2413.12	0.028(6)
		2321.18	0.021(5)
		2264.43	0.024(7)
2860.30	2723.60(36)	2650.70	0.023(6)
		2489.74	0.048(6)
2855.70	2728.20(52)	2686.72	0.057(7)
		2625.47	0.029(6)
2851.80	2732.10(42)	2732.10	0.062(11)
2849.60	2734.30(18)	2734.30	0.062(10)
		2500.44	0.027(6)
2845.50	2738.40(40)	2696.92	0.018(10)
		2635.67	0.021(8)
		2504.54	0.021(6)
2842.00	2741.90(20)	2741.90	0.056(6)
		2639.17	0.030(8)
		2508.04	0.020(6)
		2434.82	0.021(6)
2837.20	2746.70(12)	2643.97	0.053(8)
2834.10	2749.80(22)	2749.80	0.025(6)
		2676.90	0.056(6)
		2647.07	0.038(8)
2831.00	2752.90(36)	2519.04	0.016(6)
		2445.82	0.027(6)
2825.70	2758.20(29)	2524.34	0.044(6)
2822.20	2761.70(85)	2761.70	0.030(6)
2819.00	2764.90(30)	2457.82	0.026(6)
2810.00	2773.90(30)	2773.90	0.040(6)
		2732.42	0.018(6)
		2671.17	0.070(8)

E_1,keV	E_i, keV	E_2, keV	$i_{\gamma\gamma}$
		2540.04	0.022(6)
		2466.82	0.033(6)
2804.50	2779.40(30)	2545.54	0.018(6)
2801.80	2782.10(38)	2782.10	0.025(6)
		2740.62	0.023(6)
		2709.20	0.032(6)
		2679.37	0.030(6)
		2548.24	0.029(9)
		2475.02	0.023(6)
		2326.33	0.026(7)
2799.80	2784.10(44)	2550.24	0.027(9)
		2477.02	0.041(6)
2791.90	2792.00(23)	2750.52	0.015(6)
		2496.32	0.024(7)
		2484.92	0.049(6)
2786.00	2797.90(45)	2797.90	0.037(6)
		2695.17	0.087(8)
		2564.04	0.022(6)
		2490.82	0.039(6)
2778.40	2805.50(85)	2805.50	0.027(6)
		2764.02	0.082(7)
		2702.77	0.072(6)
		2349.73	0.032(6)
2772.30	2811.60(60)	2738.70	0.024(6)
		2504.52	0.029(6)
2761.10	2822.80(19)	2113.60	0.030(7)
2753.60	2830.30(45)	2727.57	0.036(6)
		2596.44	0.097(7)
2749.60	2834.30(60)	2731.57	0.042(6)
2727.60	2856.30(50)	2856.30	0.138(9)
		2753.57	0.036(6)
		2549.22	0.032(6)
2720.10	2863.80(17)	2822.32	0.041(6)

Table 1 (continued)

E_1,keV	E_i, keV	E_2, keV	$i_{\gamma\gamma}$
		2761.07	0.055(6)
		2408.03	0.082(7)
		2154.60	0.045(7)
2713.90	2870.00(22)	2870.00	0.071(8)
		2828.52	0.099(9)
		2767.27	0.190(10)
2708.10	2875.80(40)	2875.80	0.045(6)
		2773.07	0.019(6)
		2641.94	0.020(6)
2703.90	2880.00(44)	2807.10	0.027(6)
		2646.14	0.025(6)
2696.90	2887.00(61)	2814.10	0.127(9)
		2579.92	0.019(6)
		2487.98	0.028(6)
2679.80	2904.10(47)	2597.02	0.034(6)
2674.90	2909.00(92)	2909.00	0.026(8)
		2867.52	0.153(12)
		2806.27	0.116(8)
		2675.14	0.069(6)

E_1,keV	E_i, keV	E_2, keV	$i_{\gamma\gamma}$
		2601.92	0.030(7)
		2509.98	0.028(5)
2670.60	2913.30(40)	2871.82	0.037(7)
		2606.22	0.043(7)
2665.90	2918.00(31)	2918.00	0.021(6)
		2610.92	0.021(6)
2611.50	2972.40(28)	2930.92	0.121(10)
		2516.63	0.047(6)
2604.00	2979.90(29)	2938.42	0.060(7)
		2877.17	0.034(8)
2597.00	2986.90(90)	2914.00	0.025(6)
2582.20	3001.70(30)	3001.70	0.024(6)
		2898.97	0.025(6)
2577.30	3006.60(15)	3006.60	0.070(8)
		2965.12	0.026(7)
		2903.87	0.076(8)
		2772.74	0.016(6)
2573.50	3010.40(100)	3010.40	0.035(8)
		2937.50	0.042(5)

1. The lower estimation of $i_{\gamma\gamma}$ for cascades with $E_1 < 520$ keV or $E_2 < 520$ keV.
2. Only statistical uncertainty of determination of energy and intensity.

Table 2. The sum energies (keV) of cascades E_c, the calculated $I_{\gamma\gamma}^{cal}$ and experimental $I_{\gamma\gamma}^{exp}$ intensities (% per decay) of the two-step cascades in ^{193}Os.

E_c	$I_{\gamma\gamma}^{exp}$	$I_{\gamma\gamma}^{cal}$ [18,20]	$I_{\gamma\gamma}^{cal}$ [19,20]	$I_{\gamma\gamma}^{cal}$ [18,21]	$I_{\gamma\gamma}^{cal}$ [19,21]
5583.90	12.5(2)	6.2	6.5	4.7	5.3
5542.42	12.2(2)	5.6	5.7	4.4	4.7
5511.00	4.5(1)	2.9	3.0	2.2	2.5
5481.17	19.0(1)	5.1	5.3	4.0	4.4
5350.04	7.2 (2)	4.1	4.4	3.2	3.7
5288.22	3.9(2)	2.0	2.2	1.6	1.8
5276.82	8.1(4)	3.6	4.0	2.9	3.4
5184.88	4.0(2)	1.6	1.9	1.3	1.6
5128.13	3.8(2)	1.5	1.8	1.2	1.5
4874.70	1.5(1)	0.9	1.2	0.7	1.0
4694.42	3.4(2)	1.1	1.7	1.0	1.5
total	81(1)	34.6	37.7	27.2	31.4

Table 3. The energy (keV) E_c of the experimentally unresolved cascades, the energy (keV) E_f of the corresponding them final levels with the probable values of J^π for $^{191,193}Os$.

^{191}Os			^{193}Os		
E_c	E_f	J^π	E_c	E_f	J^π
5485.9	273	5/2-	5481.2	103	3/2-
5287.0	472	5/2-	5288.2	296	5/2-
5184.5	574	1/2- 3/2-	5184.9	399	5/2-
5127.9	631	5/2-	5128.1	456	5/2-

References

[1] S. T. Boneva, E. V. Vasilieva, Yu. P. Popov, A. M. Sukhovoj and V. A. Khitrov, Sov. J. Part. Nucl. **22(2)** (1991) 232;

[2] S.T. Boneva et al., Part. Nucl. **22(6)**, 698 (1991) 698;

[3] E. P. Grigoriev, V. A. Khitrov, A. M. Sukhovoj and E. V. Vasilieva Fizika B (Zagreb) **9(4)** (2000) 147;

[4] J. Honzátko et al., Nucl. Instr. and Meth. **A376**, 434 (1996)

[5] F.D. Corte, A. Simonits, in *Proceedings of International Conference on Nuclear Data for Science and Technology, Mito, 1988*, edited by S. Igarasi (Japan Atomic Energy Research Institute, 1988), 583;

[6] A.M. Sukhovoj, V.A. Khitrov, Sov. J. Prib. Tekhn. Eksp. **5**, (1984) 27;

[7] Yu.P. Popov, A. M. Sukhovoj, V. A. Khitrov and Yu. S. Yazvitsky, Izv. AN SSSR, Ser. Fiz. **48**, (1984) 891;

[8] S.T.Boneva, E.N.Vasilieva and A.M.Sukhovoj, Izv. RAN., ser. fiz., **51(11)** (1989) 2023

[9] E. Browne, Nuclear Data Sheets, 1989, **V.56**, (1989) 709;

[10] P. Fettweis and J.C. Dehaes, Z. Phys. **314**, (1983) 159;

[11] R.F. Casten et al., Nucl. Phys. **A316**, (1979) 61;

[12] Mughabghab S.F., *Neutron Cross Sections. Part B.*, NY: Academic Press 1984

[13] V.A. Bondarenko, V.A.Khitrov, A.M.Sukhovoj, J.Honzatko and I.Tomandl, JINR preprint E3-99-343, Dubna, 1999;

[14] D.Benson, Jr., P.Kleinheinz, R.K.Sheline and E.B.Shera Z.Phys. A285, (1978) 405

[15] http://www.nndc.bnl.gov/wallet/tnc/capgam.shtml

[16] A.M. Sukhovoj and V.A. Khitrov, Physics of Atomic Nuclei **62(1)**, (1999) 19;

[17] C.F. Porter and R.G. Thomas, Phys. Rev. 1956. **104**, (1956) 483;

[18] W. Dilg, W. Schantl, H. Vonach and M. Uhl, Nucl. Phys **A217** (1973) 269;

[19] A.V. Ignatyuk, Proc. of IAEA Consultants Meeting on the use of Nuclear Theory and Neutron Nuclear Data Evaluation (Trieste, 1975) IAEA-190, Vol. 1, (1976) 211;

[20] P. Axel, Phys. Rev. **126**, (1962) 683;

[21] S.G. Kadmenskij, V.P. Markushev and W.I. Furman, Yad. Fiz. **37**, (1983) 165;

[22] E. V. Vasilieva, Sukhovoj A.M. and Khitrov V.A., Phys. of Atomic Nuclei, **64(2)** (2001) 153;

[23] L.A.Malov and V.G.Soloviev, Yad. Fiz., **26(4)** (1977) 729;

[24] A.M. Sukhovoj and V.A. Khitrov, Izv. RAN, Ser. Fiz. **61(11)** (1997) 2068;

[25] E. V. Vasilieva et al., Bulletin of the Russian Academy of Science, Physics **57** (1993) 1582;

[26] S.T. Boneva et al., Phys. of Atomic Nuclei, **62(5)** (1999) 832;

Figure captions

Fig. 1. The part of the sum coincidence spectrum for $^{191,193}Os$. The peaks are labelled with the energy (in keV) of final cascade levels. The mass of the corresponding isotope is given in brackets.

Fig. 2. The part of the intensity distribution of the two-step cascades summed over 11 cascade final levels in ^{193}Os.

Fig. 3. Frequency distribution of differences of the primary transition energies E_1 of the cascades in ^{193}Os and ^{191}Os [13]. Horizontal lines represent the average value and mean-square deviation from it.

Fig. 4. The cumulative cascade intensities in ^{193}Os for four excitation energy intervals 1.50-1.75, 2.00-2.25, 2.50-2.75, and 2.75-3.00 MeV versus intensity (histograms). Approximation and extrapolation of cumulative intensities to values corresponding to $I_{\gamma\gamma} = 0$ are illustrated by solid lines.

Fig. 5. The number of the observed intermediate levels of cascades in ^{193}Os (Table 1) for the excitation energy interval of 100 keV (circles). Curves 1 and 2 represent the predictions of the models [18] and [19], respectively. The histogram is the estimation [16] of the level density from the shape of the distribution of cumulative sums of cascade intensities.

Fig. 6. The dependence of the "smoothed" intensities of resolved cascades listed in Table 1 on the excitation energy. Possible "bands" of practically harmonic excitations of the nucleus are marked. The parameter $\sigma = 25$ keV was used.

Fig. 7. The values of the functional $A(T)$ for three registration thresholds of most intense cascades. The value of the registration threshold (% per decay) is given in the figure.

Fig. 8. The value of the equidistant period T for ^{193}Os (asterisk), even-odd (triangles) and odd-odd (circles) nuclei as a function of the number of boson pairs, N_b in unfilled shells. The line represents possible dependence (drawn by eye).

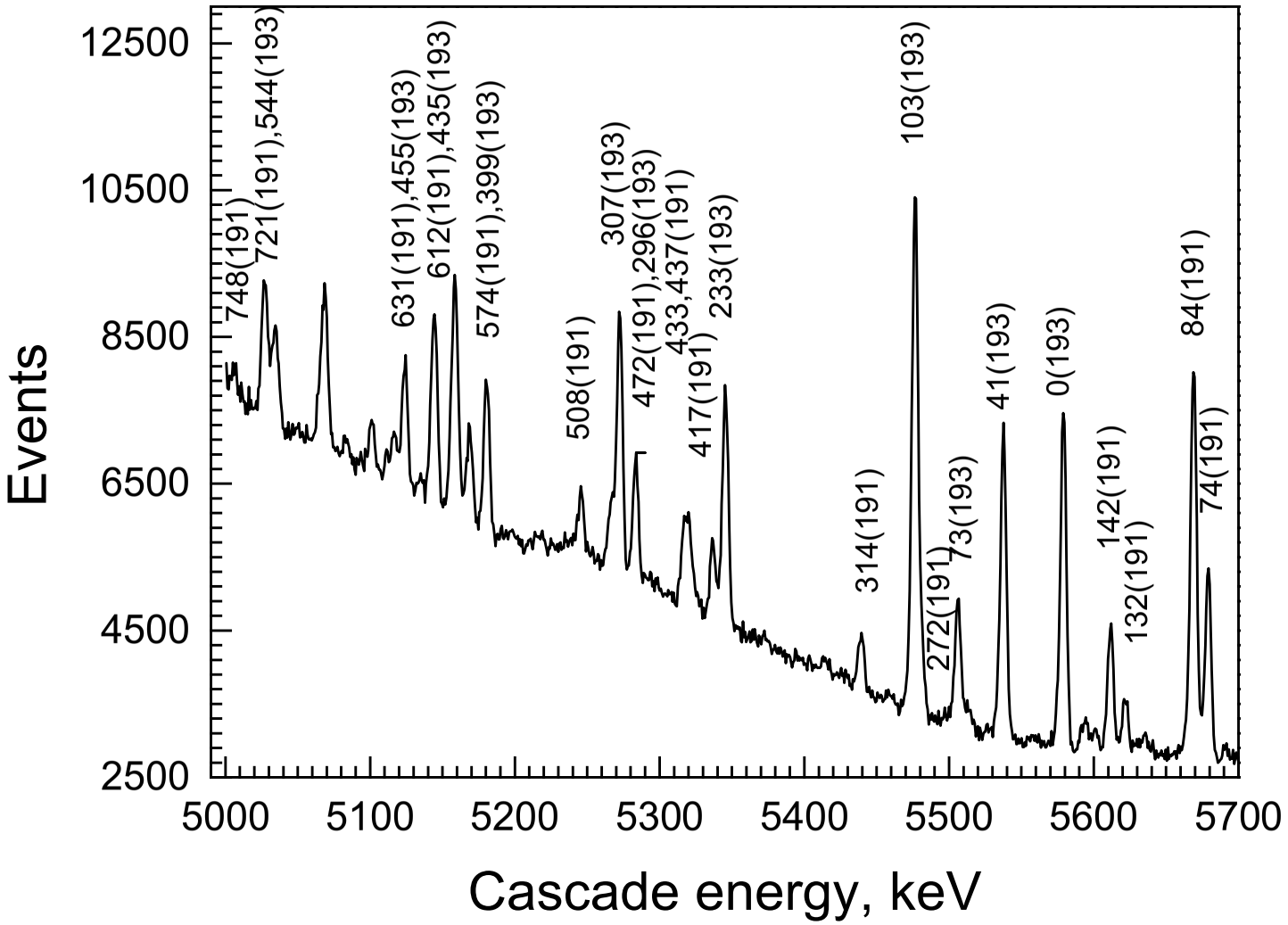
Events
12500
10500
8500
6500
4500
2500
5000
5100
5200
5300
5400
5500
5600
5700
Cascade energy, keV
748(191)
721(191),544(193)
631(191),455(193)
612(191),435(193)
574(191),399(193)
508(191)
307(193)
472(191),296(193)
433,437(191)
417(191)
233(193)
314(191)
103(193)
272(191)
73(193)
41(193)
0(193)
142(191)
132(191)
84(191)
74(191)

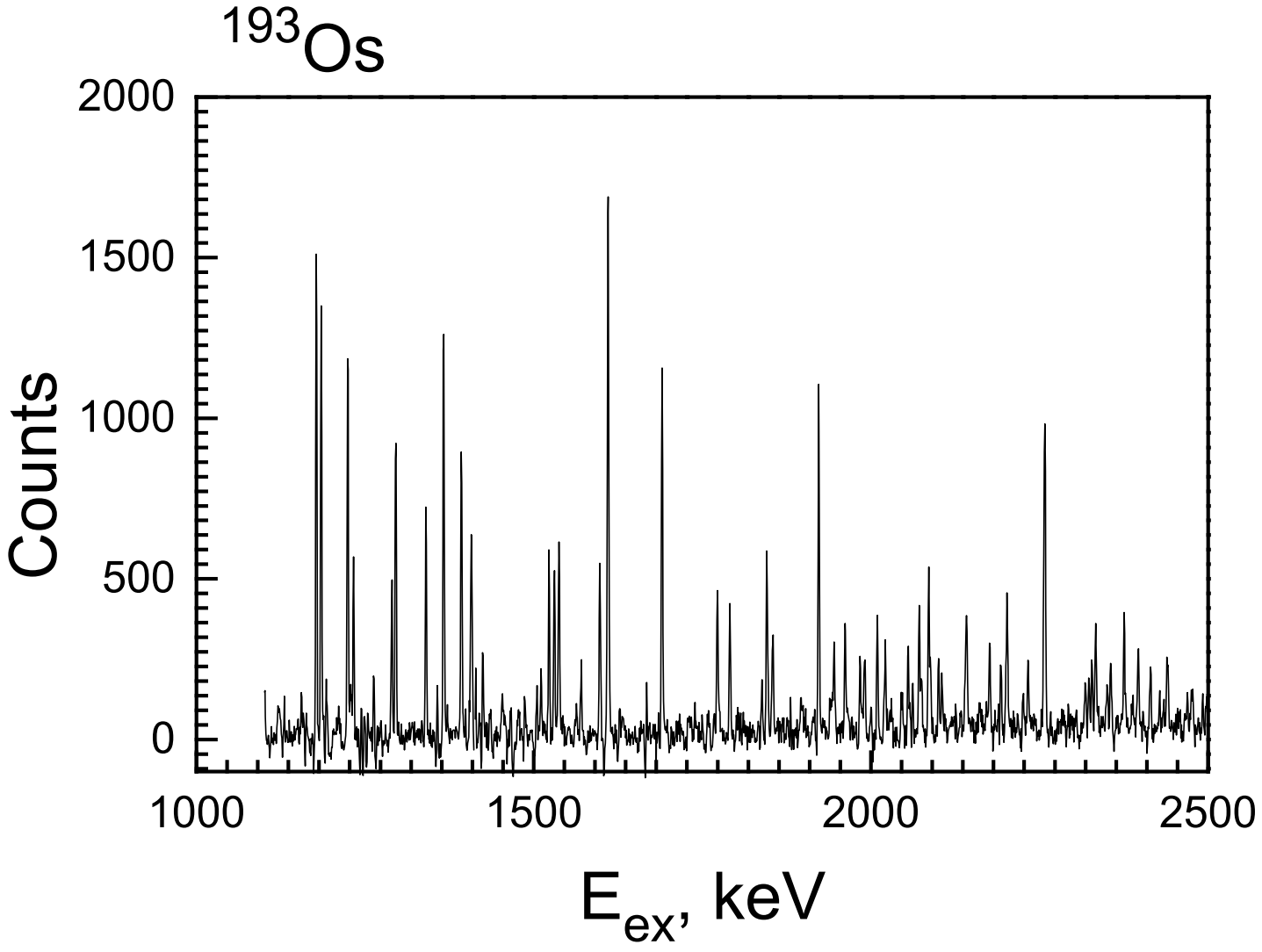
193Os
2000
1500
1000
500
0
Counts
1000
1500
2000
2500
Eex, keV

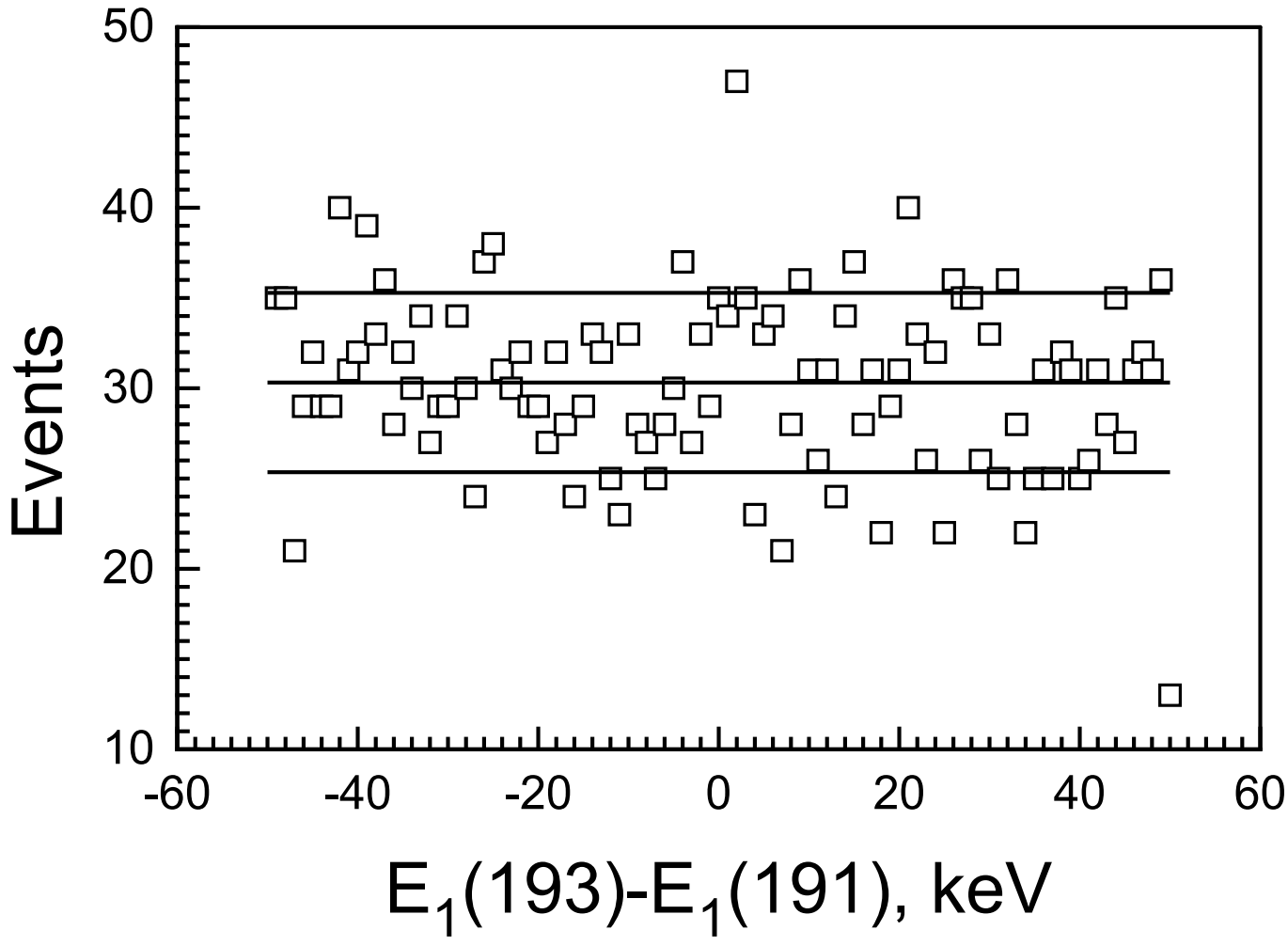
50
40
30
20
10
Events
-60
-40
-20
0
20
40
60
E1(193)-E1(191), keV

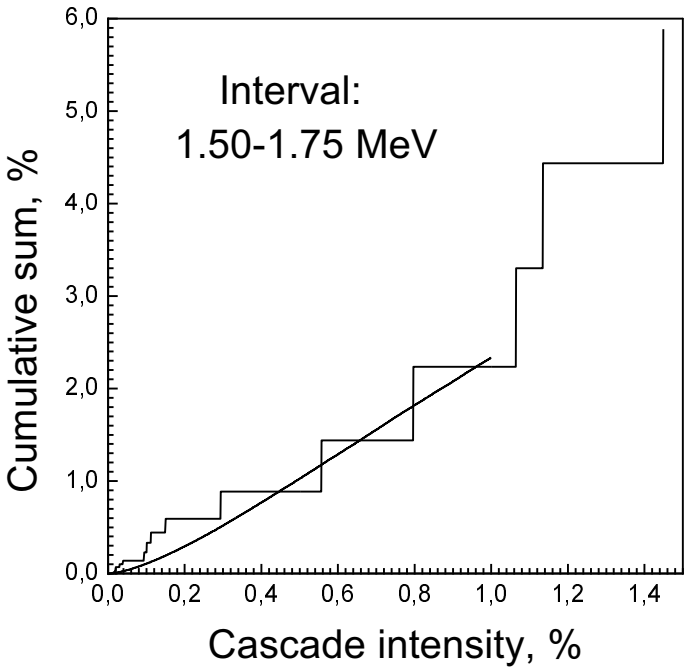
Interval:
1.50-1.75 MeV
Cumulative sum, %
Cascade intensity, %
0,0
1,0
2,0
3,0
4,0
5,0
6,0
0,2
0,4
0,6
0,8
1,2
1,4

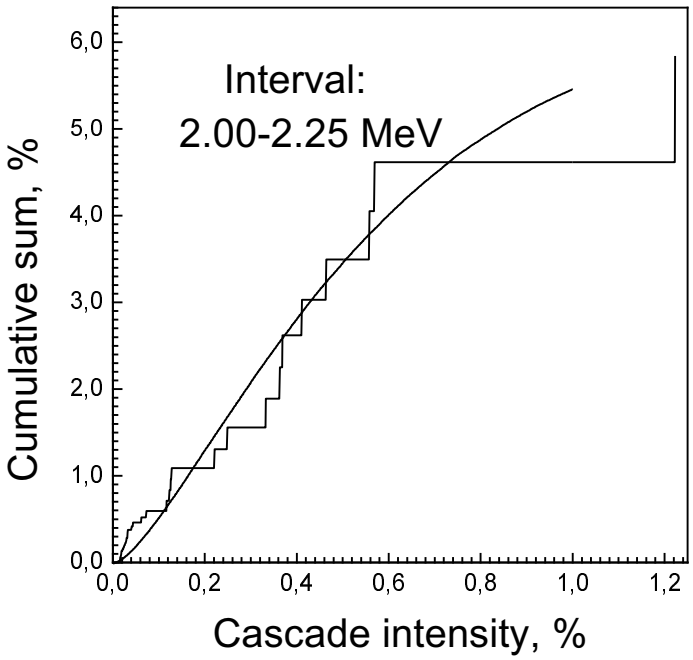
Interval:
2.00-2.25 MeV
Cumulative sum, %
Cascade intensity, %
0,0
1,0
2,0
3,0
4,0
5,0
6,0
0,2
0,4
0,6
0,8
1,0
1,2

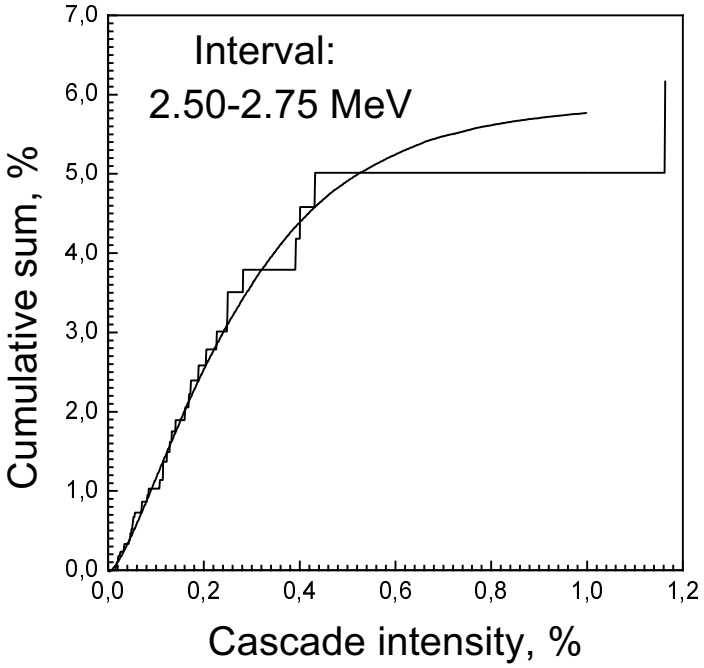
Interval:
2.50-2.75 MeV
Cumulative sum, %
Cascade intensity, %
0,0
1,0
2,0
3,0
4,0
5,0
6,0
7,0
0,2
0,4
0,6
0,8
1,0
1,2

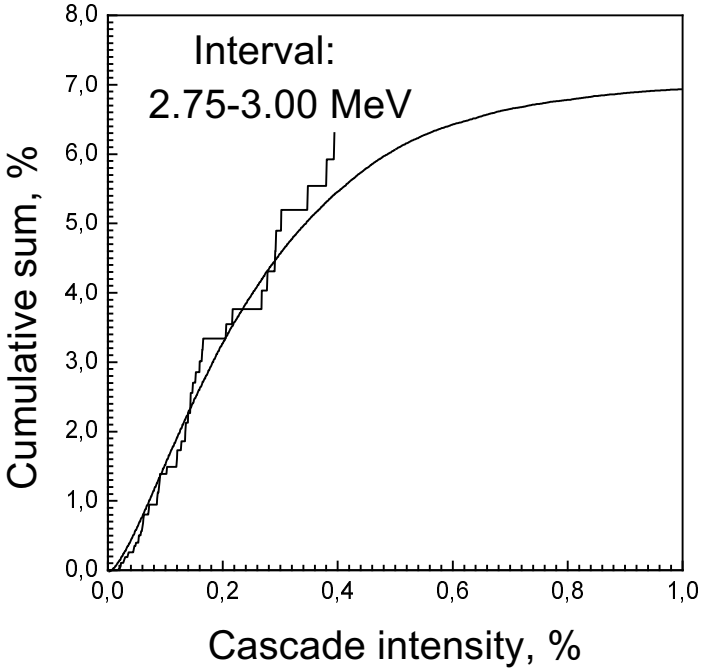
Interval:
2.75-3.00 MeV
Cumulative sum, %
Cascade intensity, %
0,0
1,0
2,0
3,0
4,0
5,0
6,0
7,0
8,0
0,2
0,4
0,6
0,8
1,0

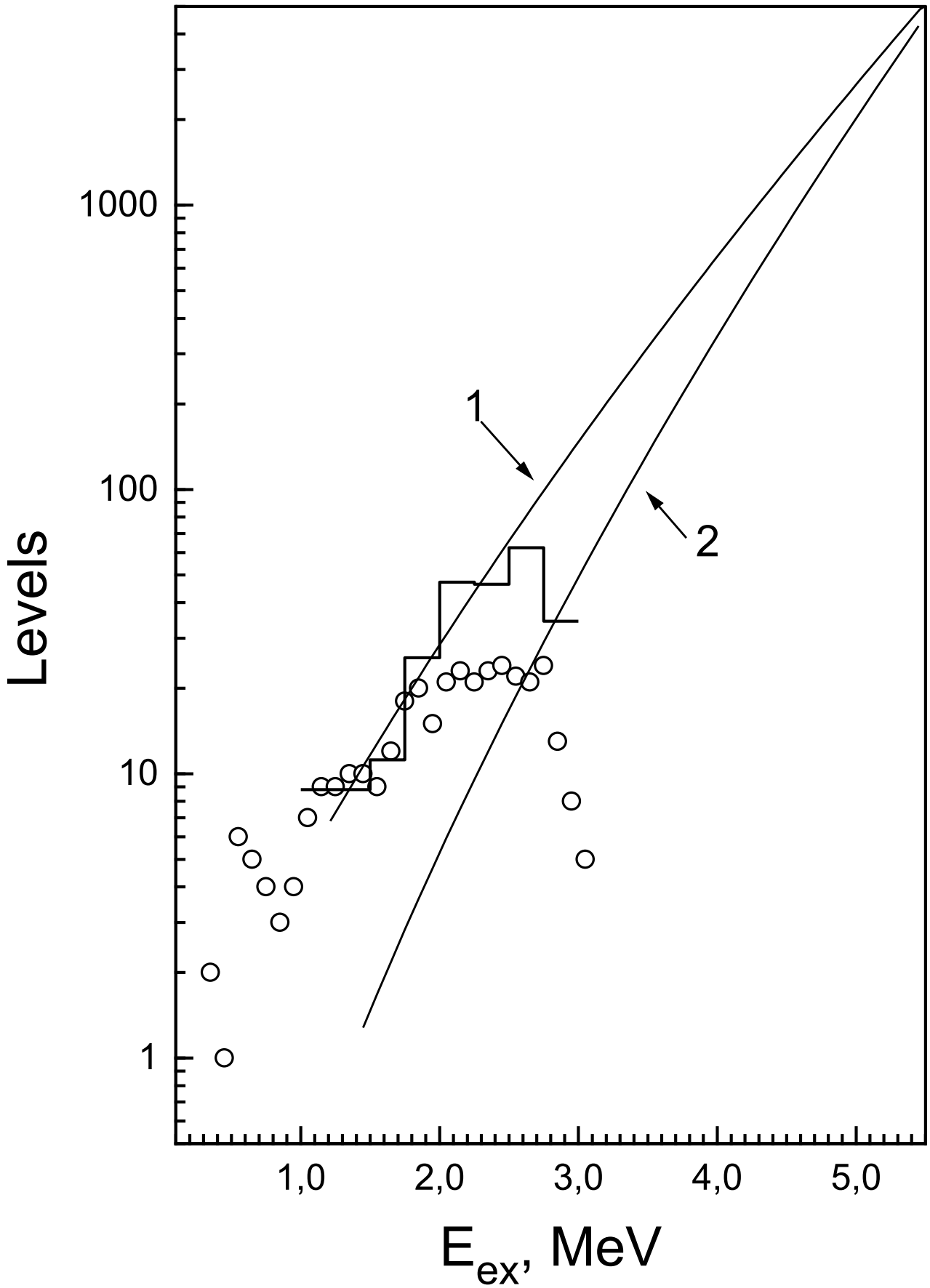
Levels
1000
100
10
1
1,0
2,0
3,0
4,0
5,0
E_ex, MeV
1
2

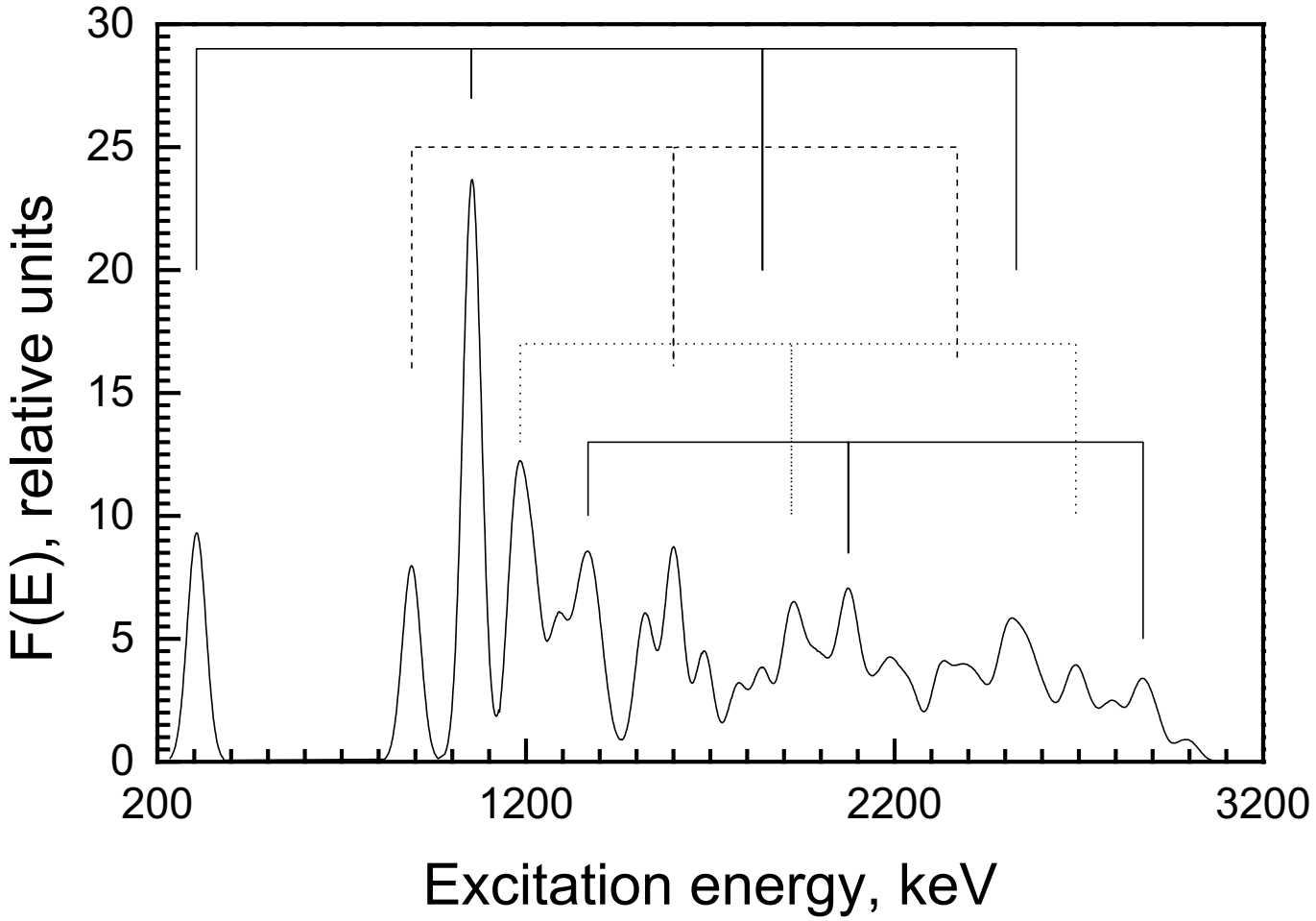
30
25
20
15
10
5
0
F(E), relative units
200
1200
2200
3200
Excitation energy, keV

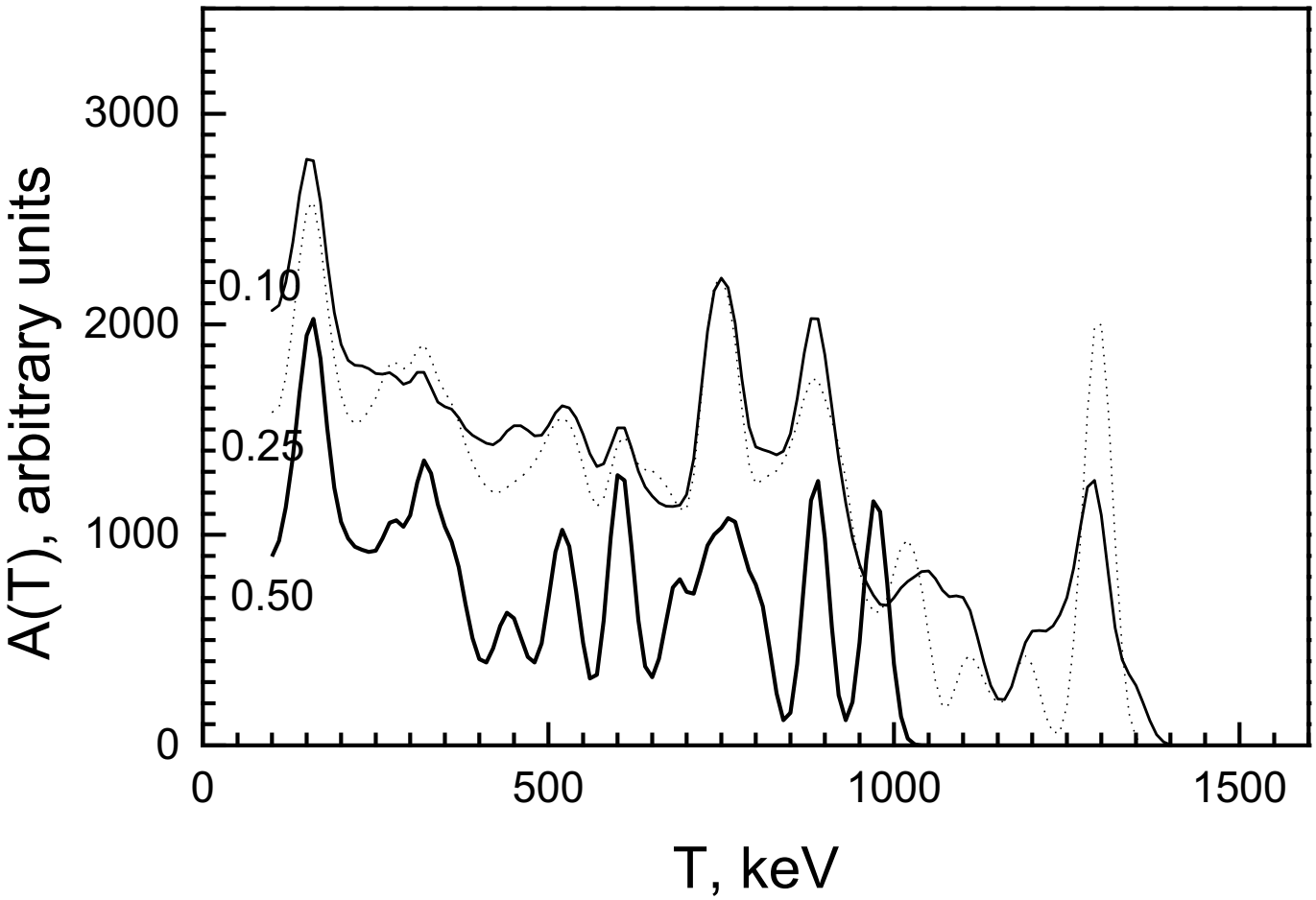
A(T), arbitrary units
T, keV
0
1000
2000
3000
0
500
1000
1500
0.10
0.25
0.50

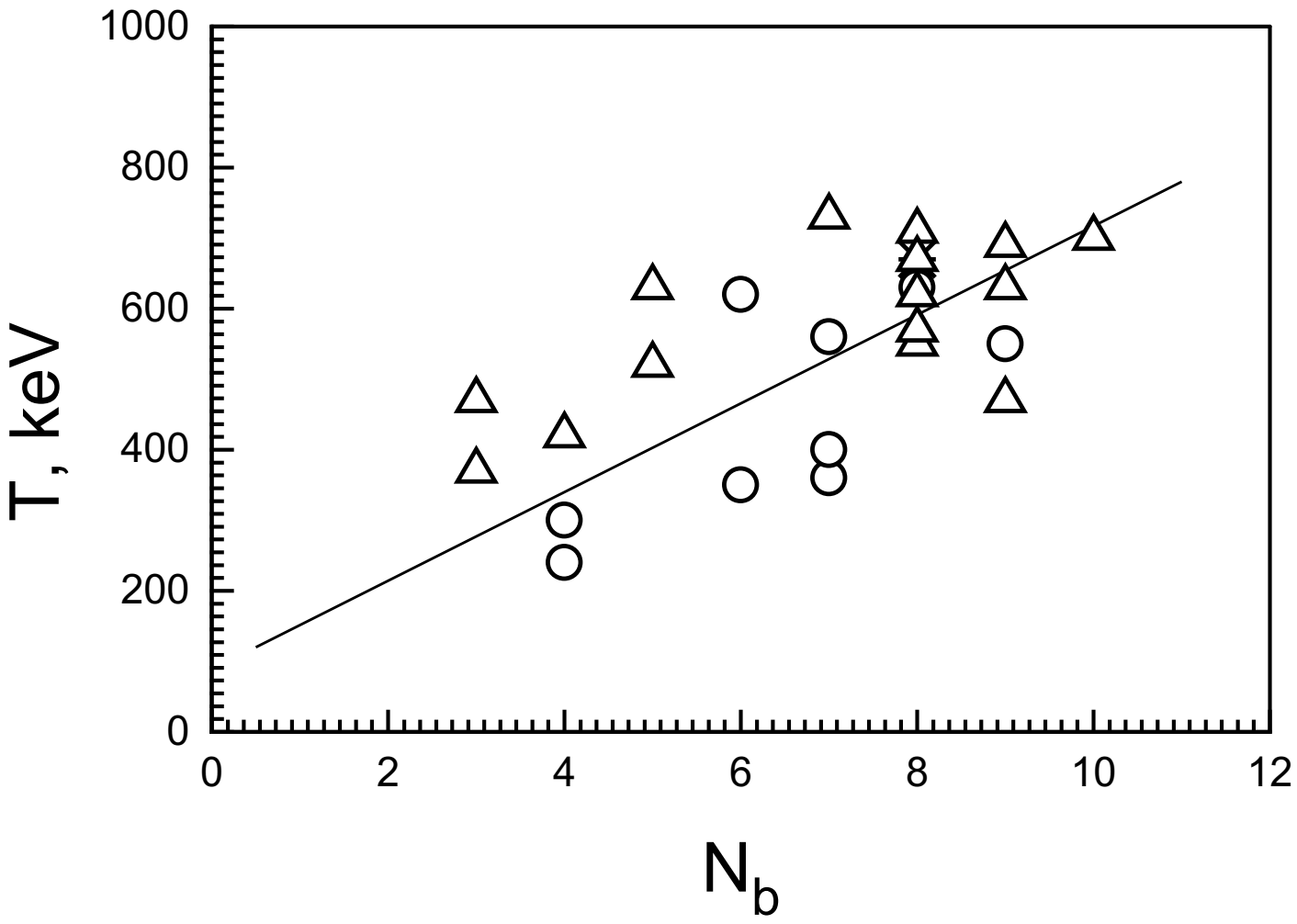
1000
800
600
400
200
0
T, keV
0
2
4
6
8
10
12
N_b